






Nontrivial retardation effects in dispersion forces: From anomalous distance dependence to novel traps

Johannes Fiedler ^{1,2,*}, Kristian Berland,³ Fabian Spallek,² Iver Brevik ⁴, Clas Persson ¹, Stefan Yoshi Buhmann ²,
and Mathias Boström ^{1,4,†}

¹Centre for Materials Science and Nanotechnology, Department of Physics, University of Oslo, P.O. Box 1048 Blindern, NO-0316 Oslo, Norway

²Physikalisches Institut, Albert-Ludwigs-Universität Freiburg, Hermann-Herder-Strasse 3, 79104 Freiburg, Germany

³Faculty of Science and Technology, Norwegian University of Life Sciences, Campus Ås Universitetstunet 3, NO-1430 Ås, Norway

⁴Department of Energy and Process Engineering, Norwegian University of Science and Technology, NO-7491 Trondheim, Norway



(Received 12 December 2019; revised manuscript received 30 April 2020; accepted 26 May 2020; published 12 June 2020)

In the study of dispersion forces, nonretarded, retarded, and thermal asymptotes with their distinct scaling laws are regarded as cornerstone results governing interactions at different separations. Here, we show that when particles interact in a medium, the influence of retardation is qualitatively different, making it necessary to consider the nonmonotonous potential in full. We discuss different regimes for several cases and find an anomalous behavior of the retarded asymptote. It can change sign and lead to a trapping potential.

DOI: [10.1103/PhysRevB.101.235424](https://doi.org/10.1103/PhysRevB.101.235424)

I. INTRODUCTION

Dispersion forces, which include the Casimir [1] and Lifshitz [2] force between two dielectric bodies, the Casimir–Polder [3] force between a dielectric body and a polarisable particle, and the London–van der Waals force [4,5] between two polarizable particles, all arise from ground-state fluctuations of the electromagnetic fields. These forces, which typically lead to an attractive interaction between the constituents, have been much studied both experimentally [6–9] and theoretically in great detail [10–12]. Systems in which dispersion forces act across a region of vacuum have received the most attention and a number of asymptotic results have been established for different geometries [13]. In most cases, a simple r^{-n} distance dependence for the nonretarded and thermal limits (with integer n) and an r^{-n-1} distance law connecting both asymptotes in the retarded regime is found. Related to this result is the fact that the proportionality constant of the nonretarded regime is larger than that from the thermal regime. When immersed in a medium [14,15], the interaction between particles is screened. For these cases, the retarded asymptote is often not a useful approximation for the full theory, at least not until it merges with the thermal asymptote. To add to the complex picture, we show here that the full interaction curves for London–van der Waals, Casimir–Polder, and Casimir–Lifshitz potentials in a medium are not always monotonically decaying, and they potentially have more than one extreme point. They can, under certain conditions, become repulsive [16,17]. Such repulsive forces can be balanced with other forces, such as buoyancy [18,19], to stabilize a particle’s position. Recently, a remarkable

Lifshitz-force induced trapping was experimentally observed exploiting a layered medium where short-range repulsion was caused by a thin-film coating, while larger distances were dominated by the underlying bulk material leading to attraction [20]. This effect was theoretically predicted earlier, e.g., by Dou *et al.* [21]. Here, we demonstrate that a dispersion potential alone, even in the absence of a layered surface, has the ability to trap particles without the presence of any balancing forces. In contrast to previous works where, for instance, retardation effects of the Casimir force have been predicted [22] or measured [23], we demonstrate that the thermal limit is more important for medium-assisted dispersion forces. Furthermore, we demonstrate that the crossings of a dielectric function may also yield a breakdown of the retarded asymptote, leading to unexpected potential behaviors.

II. MEDIUM-ASSISTED DISPERSION FORCES

In the following, we analyze the different dispersion interactions in the presence of an environmental medium with respect to their asymptotic behaviors.

A. Medium-assisted London–van der Waals interactions

The van der Waals interaction is the interaction between two neutral particles, A and B . By applying perturbation theory to the atom-field Hamiltonian [24], the energy change of the single systems can be obtained ([10], and references within),

$$U_{\text{vdW}}(\mathbf{r}_A, \mathbf{r}_B) = -\frac{\hbar\mu_0^2}{2\pi} \int_0^\infty d\xi \xi^4 \text{Tr}[\boldsymbol{\alpha}_A(i\xi) \cdot \mathbf{G}(\mathbf{r}_A, \mathbf{r}_B, i\xi) \cdot \boldsymbol{\alpha}_B(i\xi) \cdot \mathbf{G}(\mathbf{r}_B, \mathbf{r}_A, i\xi)], \quad (1)$$

which can be interpreted (reading from right to left) as the propagation of a virtual photon, which is created at particle

*johannes.fiedler@physik.uni-freiburg.de

†mathias.a.bostrom@ntnu.no

A, of frequency $i\xi$, that propagates to particle B [$\mathbf{G}(\mathbf{r}_B, \mathbf{r}_A)$], where it interacts with particle B (α_B) and is sent back to particle A , followed by the interaction with it. The sum (integral) over all these exchange processes results in the van der Waals potential.

By inserting the bulk Green's function [25],

$$\mathbf{G}(\mathbf{r}, \mathbf{r}', \omega) = -\frac{1}{3k^2} \delta(\boldsymbol{\rho}) - \frac{e^{ik\rho}}{4\pi k^2 \rho^3} \{ [1 - ik\rho - (k\rho)^2] \mathbb{I} - [3 - 3ik\rho - (k\rho)^2] \mathbf{e}_\rho \mathbf{e}_\rho \}, \quad (2)$$

with the relative coordinate $\boldsymbol{\rho} = \rho \mathbf{e}_\rho$, into Eq. (1) and applying the local-field corrections [26–28], the van der Waals potential between two particles separated by a distance ρ embedded in a medium with permittivity ε reads

$$U_{\text{vdW}}(\rho) = -\frac{\hbar}{16\varepsilon_0^2 \pi^3 \rho^6} \times \int_0^\infty d\xi \frac{\alpha_A^*(i\xi) \alpha_B^*(i\xi)}{\varepsilon^2(i\xi)} g(\xi \rho \sqrt{\varepsilon(i\xi)}/c), \quad (3)$$

with

$$g(x) = (3 + 6x + 5x^2 + 2x^3 + x^4) e^{-2x}. \quad (4)$$

In Eq. (3), $\alpha_{A,B}^*$ are the environmentally screened polarizabilities. The three standard asymptotic results for the van der Waals potential [13] between two particles are as follows:

(i) The nonretarded regime, in which $\rho n(0)$ (the optical path with refractive index at zero frequency) is significantly smaller than c/ω_{max} , with ω_{max} the largest relevant transition frequency,

$$U_{\text{vdW}}^{\text{non-ret}}(\rho) = -\frac{3\hbar}{16\varepsilon_0^2 \pi^3 \rho^6} \int_0^\infty d\xi \frac{\alpha_A^*(i\xi) \alpha_B^*(i\xi)}{\varepsilon^2(i\xi)}; \quad (5)$$

(ii) the retarded regime, in which $n(0)\rho \gg c/\omega_{\text{max}}$,

$$U_{\text{vdW}}^{\text{ret}}(\rho) = -\frac{23\hbar c}{64\varepsilon_0^2 \pi^3 \rho^7} \frac{\alpha_A^*(0) \alpha_B^*(0)}{\varepsilon^{5/2}(0)}; \quad (6)$$

(iii) the thermal limit for separations larger than the thermal wavelength $\rho n(0) \gg \hbar c/(k_B T)$, which leads to

$$U_{\text{vdW}}^{\text{th}}(\rho) = -\frac{3k_B T}{16\varepsilon_0^2 \pi^2 \rho^6} \frac{\alpha_A^*(0) \alpha_B^*(0)}{\varepsilon^2(0)}. \quad (7)$$

To illustrate how immersion in a medium (M) can affect these power laws, we consider the interaction between two spherical nanoparticles of radius a_A and a_B with response functions given by single-oscillator model dielectric functions $\varepsilon_i(i\xi) = 1 + \chi_i^{(0)}/[1 + (\xi/\omega_i)^2]$ with $i = A, B, M$ with amplitudes $\chi_A^{(0)} = 1$, $\chi_B^{(0)} = 4$, $\chi_M^{(0)} = 2$ and resonance frequencies $\omega_A = 4$ eV, $\omega_B = (1/4)$ eV, and $\omega_M = (1/2)$ eV. In this model, damping effects are neglected because its impact does not influence the potential qualitatively. The corresponding polarizabilities are computed via the Clausius–Mossotti relation [29] for interactions through a void,

$$\alpha_{\text{vac}}(\omega) = 4\pi a^3 \varepsilon_0 \frac{\varepsilon(\omega) - 1}{\varepsilon(\omega) + 2}, \quad (8)$$

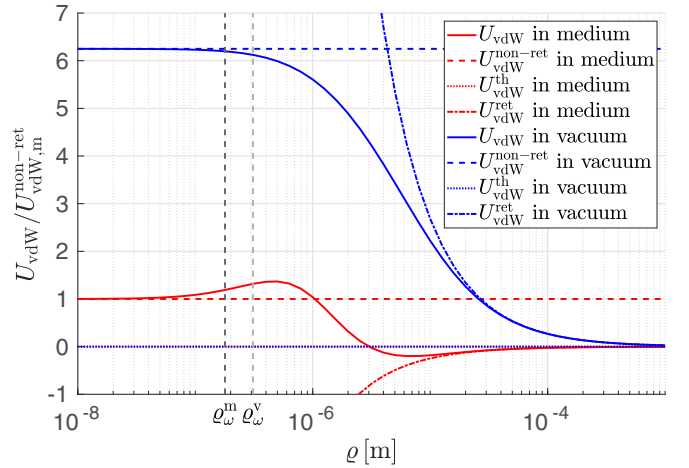


FIG. 1. The van der Waals potential normalized to the medium-assisted nonretarded limit and the corresponding asymptotes (dashed lines are the nonretarded limit, dash-dotted lines are the retarded limit, and dotted lines are the thermal limit) for a vacuum scenario (blue lines) and the corresponding case embedded in a medium (red lines).

and the hard-sphere model for interactions through a medium [27],

$$\alpha_{\text{HS}}(\omega) = 4\pi a^3 \varepsilon_0 \varepsilon_M(\omega) \frac{\varepsilon(\omega) - \varepsilon_M(\omega)}{\varepsilon(\omega) + 2\varepsilon_M(\omega)}, \quad (9)$$

with a being the particle radius.

Figure 1 shows the resulting van der Waals potentials for both the vacuum and the medium-assisted cases compared with the asymptotic expressions of Eqs. (5)–(7). For clarity, the vertical axis is scaled by the sixth power of ρ ($U_{\text{vdW},m}^{\text{non-ret}} = -C_6^m/\rho^6$). In the vacuum case (blue curves), we recover the expected limits: the exact potential follows the nonretarded asymptote for small separations ($\rho < \rho_\omega^v = c/\omega_{\text{max}}$); thereafter, it follows the retarded asymptotic form, until it finally matches the thermal limit whose amplitude is smaller than that of the nonretarded limit due to the steeper decrease in the retarded regime. This result is in agreement with the literature [23]. Depending on the optical response functions, similar results can also be found in the medium-assisted case. However, if there are crossings of the dielectric functions, the behavior of the asymptotes dramatically changes. The results for the medium-assisted case (red curves) differ drastically from these vacuum findings. First of all, retardation effects kick in at significantly shorter separations, which can be attributed to the refractive index of the medium, $\rho_\omega^m = c/[\omega_{\text{max}} n(0)]$. However, it is in the intermediate regime that a truly surprising behavior emerges. In this regime, the potential exhibits additionally distinct extreme points in the retarded regime. In fact, for this example, the retarded asymptote does not become a viable approximation for the full theory until it merges with the thermal asymptote. There is, hence, in effect no regime at all for which the retarded asymptote given by Eq. (6) gives a good description. Finally, the prefactors of the nonretarded and thermal asymptotes differ in sign. Such potential minima have been found in earlier studies, for instance in connection with surface wetting [30]; however, here we relate this to the

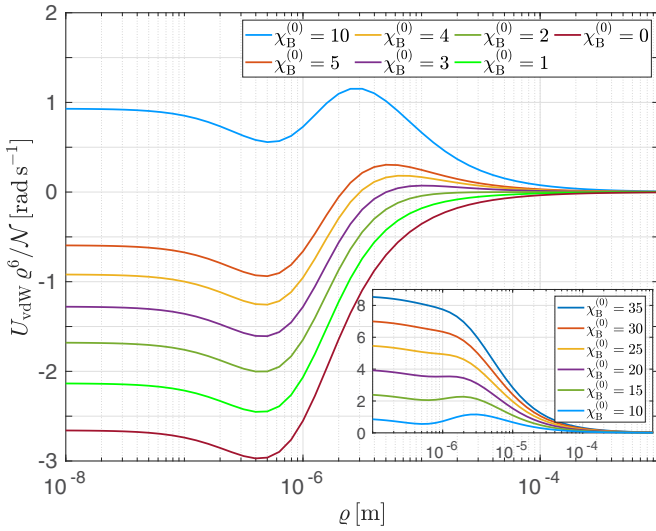


FIG. 2. Dependence of the van der Waals potential by changing the dielectric's amplitude of one material with the normalization factor $\mathcal{N} = 10^{13} \hbar \alpha_A^3 a_B^3 / \pi$. The resonances stay fixed.

breakdown of the retarded regime. In Fig. 2, we explore how adjusting the amplitude of the dielectric function of particle B affects the shape of the potential with all other parameters kept fixed, as it influences the number of intersections with the dielectric functions of the medium and particles ($\chi_B^{(0)} = 0, 1, \dots, 10, 15, 20, 25, 30, 35$). It can be observed that as $\chi_B^{(0)}$ increase, the potential changes from attraction to repulsion at short distances. For amplitudes $\chi_B^{(0)} < 2$ lower than that of the medium, only one minimum can be found according to the crossing of the dielectric function of the medium and particle. For higher values, a second extreme point at larger separation occurs due to the crossing of the dielectric functions and the lower resonant frequency of particle (ω_B) compared to that of the medium (ω_M). For very large amplitudes $\chi_B^{(0)} > 20$, the effect of the crossings vanishes and the potential becomes smoother.

B. Medium-assisted Casimir-Polder interaction

The anomalous asymptotic behavior is not restricted to particle-particle interactions. For similar crossings of dielectric functions, it can also be present for a particle with polarizability α in front of a solid plate with permittivity $\varepsilon_M(i\xi)$ at temperature T , immersed in a liquid medium with permittivity $\varepsilon_L(i\xi)$.

The Casimir-Polder interaction, in general, describes the force between a neutral particle with polarizability α in the presence of dielectric objects with permittivity $\varepsilon(\mathbf{r}, \omega)$. In analogy to the van der Waals potential, the Casimir-Polder energy can be derived via the application of perturbation theory to the atom-field Hamiltonian with a single particle [31]. The result can be written as [25]

$$U_{\text{CP}}(\mathbf{r}) = \frac{\hbar \mu_0}{2\pi} \int_0^\infty d\xi \xi^2 \text{Tr}[\alpha(i\xi) \cdot \mathbf{G}(\mathbf{r}, \mathbf{r}, i\xi)]. \quad (10)$$

By using the Green's function for planarly layered media [32],

$$\mathbf{G}(\mathbf{r}, \mathbf{r}', \omega) = \frac{i}{8\pi^2} \int \frac{d^2 k^\parallel}{k_\perp^\perp} e^{i\mathbf{k}^\parallel \cdot (\mathbf{r} - \mathbf{r}') + ik_\perp^\perp (z + z')} \times \sum_{\sigma=s,p} r_\sigma^{12} \mathbf{e}_{\sigma+}^1 \mathbf{e}_{\sigma-}^1, \quad (11)$$

with the reflection coefficients

$$r_s^{12} = \frac{k_1^\perp - k_2^\perp}{k_1^\perp + k_2^\perp}, \quad r_p^{12} = \frac{\varepsilon_2 k_1^\perp - \varepsilon_1 k_2^\perp}{\varepsilon_2 k_1^\perp + \varepsilon_1 k_2^\perp}, \quad (12)$$

again applying the local-field corrections for the excess polarizability, and introducing the temperature dependence according to the standard substitution for the integral to the Matsubara sum,

$$2\pi \hbar \int d\xi f(\xi) \mapsto k_B T \sum_{n=0}^\infty f(\xi_n) = k_B T \left[\frac{1}{2} f(\xi_0) + \sum_{n=1}^\infty f(\xi_n) \right], \quad (13)$$

with respect to the nonresonant part of the Casimir-Polder potential [33], with the primed sum denoting a sum over Matsubara frequencies $\xi_n = 2\pi n k_B T / \hbar$, with the first term weighed by 1/2 [10], the Casimir-Polder potential is given by [10]

$$U_{\text{CP}}(z_A) = \frac{k_B T \mu_0}{4\pi} \sum_{n=0}^\infty \alpha^*(i\xi_n) \xi_n^2 \times \int_0^\infty dk \frac{k}{\kappa_L^\perp} e^{-2\kappa_L^\perp z_A} \left[\frac{\kappa_L^\perp - \kappa_M^\perp}{\kappa_L^\perp + \kappa_M^\perp} - \left(1 + 2 \frac{\kappa_L^{\perp 2} c^2}{\xi_n^2 \varepsilon_L(i\xi)} \right) \frac{\varepsilon_M \kappa_L^\perp - \varepsilon_L \kappa_M^\perp}{\varepsilon_M \kappa_L^\perp + \varepsilon_L \kappa_M^\perp} \right], \quad (14)$$

with the imaginary part of the perpendicular wave vectors given by $\kappa_i^\perp = \sqrt{\varepsilon_i(i\xi) \xi^2 / c^2 + k^2}$. It takes the following forms in the nonretarded asymptote:

$$U_{\text{CP}}^{\text{non-ret}}(z) = -\frac{C_3}{z^3}, \quad (15)$$

with

$$C_3 = \frac{k_B T}{8\pi \varepsilon_0} \sum_{n=0}^\infty \frac{\alpha^*(i\xi_n) \varepsilon_M(i\xi_n) - \varepsilon_L(i\xi_n)}{\varepsilon_L(i\xi_n) \varepsilon_M(i\xi_n) + \varepsilon_L(i\xi_n)}, \quad (16)$$

and the retarded asymptote

$$U_{\text{CP}}^{\text{ret}}(z) = -\frac{C_4}{z^4}, \quad (17)$$

with

$$C_4 = \frac{3\hbar c \alpha^*(0)}{64\pi^2 \varepsilon_0 \varepsilon_L^{3/2}(0)} \int_1^\infty dv \times \left[\left(\frac{2}{v^2} - \frac{1}{v^4} \right) \frac{\varepsilon_M \sqrt{\varepsilon_L} v - \varepsilon_L \sqrt{\varepsilon_L(v^2 - 1)} + \varepsilon_M}{\varepsilon_M \sqrt{\varepsilon_L} v + \varepsilon_L \sqrt{\varepsilon_L(v^2 - 1)} + \varepsilon_M} - \frac{1}{v^4} \frac{\sqrt{\varepsilon_L} v - \sqrt{\varepsilon_L(v^2 - 1)} + \varepsilon_M}{\sqrt{\varepsilon_L} v + \sqrt{\varepsilon_L(v^2 - 1)} + \varepsilon_M} \right], \quad (18)$$

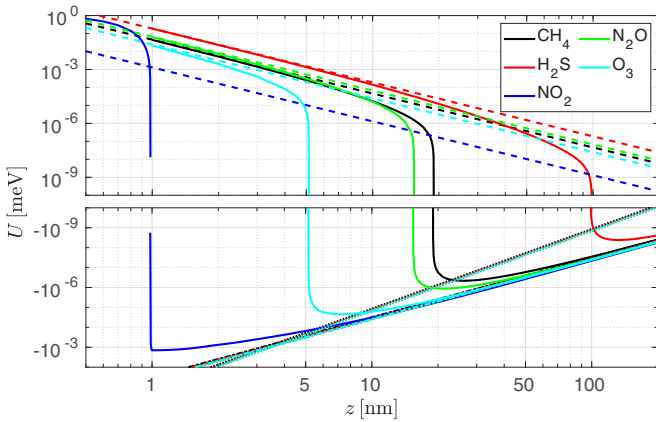


FIG. 3. The Casimir-Polder potential for dissolved CH_4 molecule (black), H_2S (red), NO_2 (blue), N_2O (green), and O_3 (cyan) near the water surface shown together with the two limiting asymptotes: nonretarded (dashed line) and retarded (dotted line).

and, finally, in the thermal limit, it is given by

$$U_{\text{CP}}^{\text{th}}(z) = -\frac{C_{3\text{T}}}{z^3}, \quad (19)$$

with

$$C_{3\text{T}} = -\frac{k_{\text{B}}T}{16\pi\epsilon_0} \frac{\alpha^*(0)\epsilon_{\text{M}}(0) - \epsilon_{\text{L}}(0)}{\epsilon_{\text{L}}(0)\epsilon_{\text{M}}(0) + \epsilon_{\text{L}}(0)}. \quad (20)$$

The behavior of the three asymptotes in vacuum is similar to the previously discussed van der Waals case depicted in Fig. 1, with modified power laws (r^{-3} for nonretarded, r^{-4} for retarded, and r^{-3} for the thermal asymptote). Further details can be found in Ref. [34].

Applying this model to a specific example, we consider greenhouse gases with polarizabilities, and particle and cavity radii taken from Ref. [27]. The gases immersed in water interact with the water-air interface. Further, we use the finite-size model of Refs. [26,27] to describe the excess polarizability that arises when taking into account the finite-size effects of the particles and a vacuum layer surrounding the particle to avoid the contact between particle and solvent [35]. The calculated potentials and the corresponding asymptotes are depicted in Fig. 3. The corresponding parameters for the asymptotes, trapping distances, and frequencies are given in Table I. It can be observed that hydrogen sulfide ($z_{\text{trap}} = 132$ nm), methane (26 nm), nitrogen dioxide (21 nm), ozone (7 nm), and nitrous oxide (1 nm) are trapped near the surface. For these systems, a potential minimum occurs between the nonretarded and thermal limits and the retarded limit does not appear as an r^{-4} power law. Some correlation between the trapping distance z_{trap} and the position corresponding to the change in sign of the dielectric function $z_0 = c/[\omega_0 n(0)]$ with $\alpha(i\omega_0) = 0$ can be found, as well as between the trapping distance and the transition distance between the retarded and nonretarded limit z_ω . However, a simple correlation between one of them alone and the trapping distances cannot be expected because the potential depends on all three quantities: the dielectric functions of the medium and the polarizabilities of the particles, whereas each of these parameters only depends on one of them. The gas molecule H_2S deviates from

TABLE I. Data of C_3 coefficients [$\mu\text{eV}(\text{nm})^3$] [Eq. (16)], C_4 coefficients [$\mu\text{eV}(\text{nm})^4$] [Eq. (18)], $C_{3\text{T}}$ coefficients [$\mu\text{eV}(\text{nm})^3$] [Eq. (20)], trapping distances [z_{trap} (nm)], and the corresponding trapping frequency [ω_{trap} (MHz)] for different molecules dissolved in water at $T = 273.16$ K near a water-air surface. Positive C_3 , C_4 , and $C_{3\text{T}}$ values correspond to attraction. Further, the distances for the impact of retardation [z_ω (nm)] are given for each case. The thermal effects occur on distances larger than $z_{\text{T}} = 893$ nm. As an approximation of the trapping distance, the table shows the values for z_0 that correspond to the roots of the polarizabilities.

Mol.	C_3	C_4	$C_{3\text{T}}$	z_{trap}	z_0	z_ω	ω_{trap}
CH_4	-45.9	11638	31.3	26.0	59.2	1.0	6.5
CO	109.9	12755	34.3		0.8	0.2	
CO_2	31.3	15464	41.6		2.4	0.3	
H_2S	-189.9	12958	34.8	132.1	142.1	2.2	0.1
N_2	66.4	11181	30.1		1.5	0.3	
NO_2	-1.3	14466	38.9	1.0	3.6	0.3	3930
N_2O	-66.8	14574	39.2	21.0	41.4	0.5	7.8
O_2	96.4	10903	29.3		1.1	0.2	
O_3	-24.9	14562	39.2	7.2	26.0	0.3	90.8

most other gas molecules in the nonretarded limit in having a very large negative C_3 in Table I. One would have expected H_2S to be hydrophobic, as was recently discussed in Ref. [36]. This result will require further investigation.

By comparing the depth of the potential minimum with the thermal energy, one finds that the stability of the trap is given at temperatures far below the freezing temperature of water. This means that for these examples, the interactions are not strong enough to trap particles. In terms of particles dissolved in a medium, one might be able to discern a slightly higher concentration of particles at these specific trapping distances. We note that the thermal stability of the trap increases with decreasing trap distance. Further, the energetic minimum of the potential becomes steeper with decreasing trap distance, resulting in a narrowed trapping potential the closer it gets to the interface. For different materials, these trends will be similar.

Single gas molecules reveal anomalous interactions near a water surface, but the typical energy minimum is not sufficiently deep to act as an effective trap. Inspired by the observed Casimir-Polder repulsion for air bubbles in water near solid surfaces [16,37] we consider a system where we expect trapping could occur. Specifically, we consider an air bubble dissolved in liquid bromobenzene [17] in front of a horizontal or vertical amorphous silica surface. For modeling, we used parameters corresponding to amorphous silica (volume of the SiO_2 unit: $V_v = 41.14 \text{ \AA}^3$ [38]) at room temperature ($T = 298$ K). Due to a crossing of dielectric functions for amorphous silica and bromobenzene at a specific frequency, the air bubble can be trapped via short-range repulsive and long-range attractive Casimir-Lifshitz forces [10]. Here, we apply a simple version of the Derjaguin approximation to estimate the force on the sphere of radius R , $f_{\text{sphere}}(x) = 2\pi R U_{\text{plane}}(x)$ with $U_{\text{plane}}(x)$ being the energy for the planar system. We then integrate the force from infinity up to the specific distance x to obtain the interaction free energy acting on a sphere at a distance x from the planar interface. The minimum sphere radius

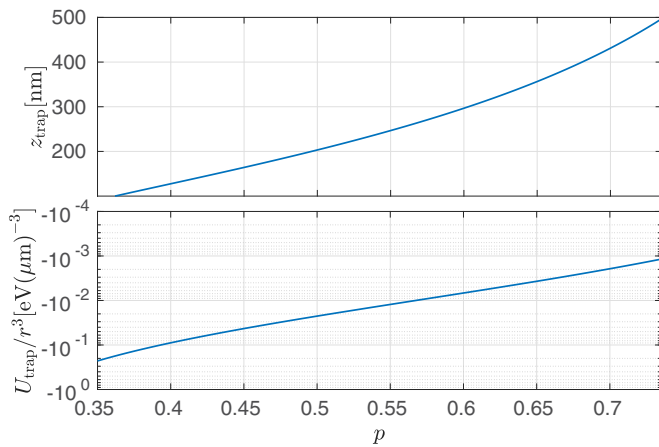


FIG. 4. Trap parameters depending on the volume fraction p .

R_{\min} will be estimated from the size that provides a trapping energy larger than or equal to $k_B T$. Here, we find an estimate for a thermally stable position of approximately 7 nm in front of the surface for bubbles with a radius much larger than $R_{\min} = 200$ nm. Hence, we are in a range for relative sizes and distances where the Derjaguin approximation is appropriate to use, but where surface roughness and various other nanoscale effects are important. The short-range repulsion experienced by the typical air bubble is expected to lead to low surface friction. We note that for bubbles below or above a surface, there will also be some influence on trapping distance from buoyancy, $b = Vg(\rho_l - \rho_a)$, which depends on volume (V), gravitational constant g , and the difference in mass density for bubble ρ_a and the liquid ρ_l . However, in front of a vertical surface, buoyancy only acts to move the air bubble upwards, while the proposed mechanism keeps it moving with low friction at a fixed trapping distance from the surface.

III. APPLICATION: TUNEABLE TRAP

Ideally, a larger trapping distance than found above would be more realistic for experimental realization. Thus, to introduce a scalable parameter for tuning the trap, we consider in our final example a two-component fluid surrounding the particle. For the dielectric functions of mixtures between fluid 1 (ϵ_1) and fluid 2 (ϵ_2), we use a Lorentz-Lorenz model [19,39,40], where we introduce the volume fraction p of fluid 1 in fluid 2. We chose the liquids bromobenzene and methanol in front of a polystyrene surface [17] as the dielectric function of the latter lies between both fluids. An illustration of the

resulting dielectric functions can be found in Ref. [41]. In this case, the crossings of the dielectric functions depend on the volume fraction. We used the example of an anatase-TiO₂ spherical nanoparticle whose dielectric function was taken from Ref. [42]. As we consider larger particles compared to few-atomic molecules from the example above, we describe the excess polarizability via the hard-sphere model as in the introductory van der Waals example. The resulting parameters for the trap are given in Fig. 4. We predict that the trapping can be tuned over a wide range of distances (100–500 nm) by changing the liquid mixture.

IV. RESULTS AND CONCLUSION

To conclude, we have shown that the impact of retardation dramatically changes the asymptotic behavior of dispersion interactions in media. In contrast to the ordinary theory in vacuum, the retarded power laws are not applicable and a consideration of the full interaction potential is required instead. Further, the transition distance between nonretarded and retarded regimes strongly decreases by immersing the interacting particles in a liquid due to its refractive index. This extends previous work on Casimir–Lifshitz forces in fluids (see, e.g., Refs. [2,17,19,20,23,30,43]) to a more general case where retarded dispersion forces can reveal a very complex behavior in media. For this reason, considerations of retardation effects are important for medium-assisted dispersion force experiments, for example, Casimir experiments [16,23,43], medium-assisted optical tweezers [44], colloidal systems [45], and in future measurements of the Casimir torque in a medium [46,47]. Beyond these impacts, we have shown that the near-field effect of dispersion forces in colloidal system yields an inhomogeneous particle density distribution near interfaces due to trapping potentials. The introduced mechanism can, for instance, be used to trap nanoparticles at low temperature, specifically nanodiamonds [48], by choosing liquid nitrogen, liquid fluorine, or atomic clouds as an environmental medium. The presented theory is more general and can be applied to several systems beyond Casimir experiments, especially medium-assisted spectroscopy in nanodroplets [49–51].

ACKNOWLEDGMENTS

We acknowledge support from the Research Council of Norway (Project No. 250346). We gratefully acknowledge support by the German Research Council Grants No. BU 1803/6-1 (S.Y.B. and J.F.) and No. BU 1803/3-1 (S.Y.B. and F.S.).

- [1] H. B. G. Casimir, On the attraction between two perfectly conducting plates, *K. Ned. Akad. Wet.* **51**, 793 (1948).
- [2] I. Dzyaloshinskii, E. Lifshitz, and L. Pitaevskii, The general theory of van der Waals forces, *Adv. Phys.* **10**, 165 (1961).
- [3] H. B. G. Casimir and D. Polder, The influence of retardation on the London–van der Waals forces, *Phys. Rev.* **73**, 360 (1948).

- [4] F. London, Zur Theorie und Systematik der Molekularkräfte, *Z. Phys.* **63**, 245 (1930).
- [5] J. D. van der Waals, Over de Continuïteit van den Gas- en Vloeïstoftoestand, Ph.D. dissertation, University Leiden, 1873.
- [6] D. Ebeling, M. Šekutor, M. Stieffermann, J. Tschakert, J. E. P. Dahl, R. M. K. Carlson, A. Schirmeisen, and P. R. Schreiner, London dispersion directs on-surface self-assembly of [121]tetramantane molecules, *ACS Nano* **11**, 9459 (2017).

- [7] W. Schöllkopf and J. P. Toennies, Nondestructive mass selection of small van der Waals clusters, *Science* **266**, 1345 (1994).
- [8] R. E. Grisenti, W. Schöllkopf, J. P. Toennies, G. C. Hegerfeldt, and T. Köhler, Determination of Atom-Surface Van der Waals Potentials from Transmission-Grating Diffraction Intensities, *Phys. Rev. Lett.* **83**, 1755 (1999).
- [9] M. Arndt, O. Nairz, J. Vos-Andreae, C. Keller, G. van der Zouw, and A. Zeilinger, Wave-particle duality of C_{60} molecules, *Nature (London)* **401**, 680 (1999).
- [10] S. Y. Buhmann, *Dispersion Forces I: Macroscopic Quantum Electrodynamics and Ground-State Casimir, Casimir-Polder and Van Der Waals Forces*, Springer Tracts in Modern Physics (Springer, Heidelberg, 2012).
- [11] D. Dalvit, P. Milonni, D. Roberts, and F. da Rosa, *Casimir Physics*, Lecture Notes in Physics (Springer, Heidelberg, 2011).
- [12] N. Cherroret, R. Guérou, A. Lambrecht, and S. Reynaud, Statistical approach to Casimir-Polder potentials in heterogeneous media, *Phys. Rev. A* **92**, 042513 (2015).
- [13] S. Y. Buhmann, S. Scheel, and J. Babington, Universal Scaling Laws for Dispersion Interactions, *Phys. Rev. Lett.* **104**, 070404 (2010).
- [14] D. S. Ether, L. B. Pires, S. Umrath, D. Martinez, Y. Ayala, B. Pontes, G. R. de S. Araújo, S. Frases, G.-L. Ingold, F. S. S. Rosa, N. B. Viana, H. M. Nussenzeig, and P. A. M. Neto, Probing the Casimir force with optical tweezers, *Europhys. Lett.* **112**, 44001 (2015).
- [15] P. Loskill, H. Hähl, T. Faidt, S. Grandthyll, F. Müller, and K. Jacobs, Is adhesion superficial? Silicon wafers as a model system to study van der Waals interactions, *Adv. Colloid Interface Sci.* **179–182**, 107 (2012).
- [16] R. F. Tabor, R. Manica, D. Y. C. Chan, F. Grieser, and R. R. Dagastine, Repulsive van der Waals Forces in Soft Matter: Why Bubbles Do Not Stick to Walls, *Phys. Rev. Lett.* **106**, 064501 (2011).
- [17] P. J. van Zwol and G. Palasantzas, Repulsive Casimir forces between solid materials with high-refractive-index intervening liquids, *Phys. Rev. A* **81**, 062502 (2010).
- [18] P. Thiyam, J. Fiedler, S. Y. Buhmann, C. Persson, I. Brevik, M. Boström, and D. F. Parsons, Ice particles sink below the water surface due to a balance of salt, van der waals, and buoyancy forces, *J. Phys. Chem. C* **122**, 15311 (2018).
- [19] M. Boström, M. Dou, O. I. Malyi, P. Parashar, D. F. Parsons, I. Brevik, and C. Persson, Fluid-sensitive nanoscale switching with quantum levitation controlled by α -Sn/ β -Sn phase transition, *Phys. Rev. B* **97**, 125421 (2018).
- [20] R. Zhao, L. Li, S. Yang, W. Bao, Y. Xia, P. Ashby, Y. Wang, and X. Zhang, Stable Casimir equilibria and quantum trapping, *Science* **364**, 984 (2019).
- [21] M. Dou, F. Lou, M. Boström, I. Brevik, and C. Persson, Casimir quantum levitation tuned by means of material properties and geometries, *Phys. Rev. B* **89**, 201407(R) (2014).
- [22] M. Boström, S. A. Ellingsen, I. Brevik, D. F. Parsons, and B. E. Sernelius, Sign of the casimir-polder interaction between atoms and oil-water interfaces: Subtle dependence on dielectric properties, *Phys. Rev. A* **85**, 064501 (2012).
- [23] M. A. Bevan and D. C. Prieve, Direct measurement of retarded van der Waals attraction, *Langmuir* **15**, 7925 (1999).
- [24] H. Safari, S. Y. Buhmann, D.-G. Welsch, and H. T. Dung, Body-assisted van der Waals interaction between two atoms, *Phys. Rev. A* **74**, 042101 (2006).
- [25] S. Scheel and S. Buhmann, Macroscopic quantum electrodynamics - Concepts and applications, *Act. Phys. Slov.* **58**, 675 (2008).
- [26] A. Sambale, S. Y. Buhmann, D.-G. Welsch, and M.-S. Tomaš, Local-field correction to one- and two-atom van der Waals interactions, *Phys. Rev. A* **75**, 042109 (2007).
- [27] J. Fiedler, P. Thiyam, A. Kurumbail, F. A. Burger, M. Walter, C. Persson, I. Brevik, D. F. Parsons, M. Boström, and S. Y. Buhmann, Effective polarizability models, *J. Phys. Chem. A* **121**, 9742 (2017).
- [28] F. A. Burger, J. Fiedler, and S. Y. Buhmann, Zero-point electromagnetic stress tensor for studying Casimir forces on colloidal particles in media, *Europhys. Lett.* **121**, 24004 (2018).
- [29] J. D. Jackson, *Classical Electrodynamics*, 3rd ed. (Wiley, New York, 1999).
- [30] M. Elbaum and M. Schick, Application of the Theory of Dispersion Forces to the Surface Melting of Ice, *Phys. Rev. Lett.* **66**, 1713 (1991).
- [31] S. Y. Buhmann, H. T. Dung, and D.-G. Welsch, The van der Waals energy of atomic systems near absorbing and dispersing bodies, *J. Opt. B: Quantum Semiclass. Opt.* **6**, S127 (2004).
- [32] M. S. Tomaš, Green function for multilayers: Light scattering in planar cavities, *Phys. Rev. A* **51**, 2545 (1995).
- [33] S. Y. Buhmann, *Dispersion Forces II: Many-Body Effects, Excited Atoms, Finite Temperature and Quantum Friction*, Springer Tracts in Modern Physics (Springer, Heidelberg, 2012).
- [34] S. Y. Buhmann, S. Scheel, S. A. Ellingsen, K. Hornberger, and A. Jacob, Casimir-Polder interaction of Fullerene molecules with surfaces, *Phys. Rev. A* **85**, 042513 (2012).
- [35] A. Held and M. Walter, Simplified continuum solvent model with a smooth cavity based on volumetric data, *J. Chem. Phys.* **141**, 174108 (2014).
- [36] J. Fiedler, M. Boström, C. Persson, I. Brevik, R. Corkery, S. Y. Buhmann, and D. F. Parsons, Full-spectrum high-resolution modeling of the dielectric function of water, *J. Phys. Chem. B* **124**, 3103 (2020).
- [37] V. Esteso, S. Carretero-Palacios, P. Thiyam, H. Miguez, D. F. Parsons, I. Brevik, and M. Boström, Trapping of gas bubbles in water at a finite distance below a water–solid interface, *Langmuir* **35**, 4218 (2019).
- [38] O. I. Malyi, M. Boström, V. V. Kulish, P. Thiyam, D. F. Parsons, and C. Persson, Volume dependence of the dielectric properties of amorphous SiO_2 , *Phys. Chem. Chem. Phys.* **18**, 7483 (2016).
- [39] D. E. Aspnes, Local-field effects and effective-medium theory: A microscopic perspective, *Am. J. Phys.* **50**, 704 (1982).
- [40] M. Boström, R. W. Corkery, E. R. A. Lima, O. I. Malyi, S. Y. Buhmann, C. Persson, I. Brevik, D. F. Parsons, and J. Fiedler, Dispersion forces stabilize ice coatings at certain gas hydrate interfaces that prevent water wetting, *ACS Earth Space Chem.* **3**, 1014 (2019).
- [41] J. Fiedler, C. Persson, and S. Y. Buhmann, Spectroscopy of Nanoparticles without Light, *Phys. Rev. Appl.* **13**, 014025 (2020).

- [42] M. Dou and C. Persson, Comparative study of rutile and anatase SnO_2 and TiO_2 : Band-edge structures, dielectric functions, and polaron effects, *J. Appl. Phys.* **113**, 083703 (2013).
- [43] J. N. Munday, F. Capasso, V. A. Parsegian, and S. M. Bezrukov, Measurements of the Casimir-Lifshitz force in fluids: The effect of electrostatic forces and Debye screening, *Phys. Rev. A* **78**, 032109 (2008).
- [44] D. Gao, W. Ding, M. Nieto-Vesperinas, X. Ding, M. Rahman, T. Zhang, C. Lim, and C.-W. Qiu, Optical manipulation from the microscale to the nanoscale: Fundamentals, advances and prospects, *Light Sci. Applic.* **6**, e17039 (2017).
- [45] G. Brügger, L. S. Froufe-Pérez, F. Scheffold, and J. José Sáenz, Controlling dispersion forces between small particles with artificially created random light fields, *Nat. Commun.* **6**, 7460 (2015).
- [46] D. A. T. Somers and J. N. Munday, Casimir-Lifshitz Torque Enhancement by Retardation and Intervening Dielectrics, *Phys. Rev. Lett.* **119**, 183001 (2017).
- [47] P. Thiyam, P. Parashar, K. V. Shajesh, O. I. Malyi, M. Boström, K. A. Milton, I. Brevik, J. Forsman, and C. Persson, Effect of excess charge carriers and fluid medium on the magnitude and sign of the Casimir-Lifshitz torque, *Phys. Rev. B* **100**, 205403 (2019).
- [48] Y. Dumeige, J.-F. Roch, F. Bretenaker, T. Debuisschert, V. Acosta, C. Becher, G. Chatzidrosos, A. Wickenbrock, L. Bougas, A. Wilzewski, and D. Budker, Infrared laser threshold magnetometry with a NV doped diamond intracavity etalon, *Opt. Express* **27**, 1706 (2019).
- [49] M. Dvorak, M. Müller, T. Knoblauch, O. Bünermann, A. Rydlo, S. Minniberger, W. Harbich, and F. Stienkemeier, Spectroscopy of 3, 4, 9, 10-perylenetetracarboxylic dianhydride (PTCDA) attached to rare gas samples: Clusters vs. bulk matrices. I. Absorption spectroscopy, *J. Chem. Phys.* **137**, 164301 (2012).
- [50] M. Kelbg, A. Heidenreich, L. Kazak, M. Zabel, B. Krebs, K.-H. Meiwes-Broer, and J. Tiggesbäumker, Comparison of electron and ion emission from xenon cluster-induced ignition of helium nanodroplets, *J. Phys. Chem. A* **122**, 8107 (2018).
- [51] O. Stauffert, S. Izadnia, F. Stienkemeier, and M. Walter, Optical signatures of pentacene in soft rare-gas environments, *J. Chem. Phys.* **150**, 244703 (2019).